

Cite this: *Anal. Methods*, 2025, 17, 7799

Fast and sustainable active pharmaceutical ingredient (API) screening in over-the-counter and prescription drug products by surface-assisted plasma-based desorption/ionization high-resolution mass spectrometry

Maximilian Heide,^a Jonas Reifenrath,^a Alexander Herrmann^a
and Carsten Engelhard^{*abc}

Fast chemical analysis of pharmaceutical preparations is important for quality assurance, counterfeit drug detection, and consumer health. While quantitative methods such as high-performance liquid chromatography mass spectrometry (HPLC-MS) are powerful, there is a need for sustainable and environmentally friendly methods, which require less chemicals and produce less waste. Here, solvent-free ambient desorption/ionization (ADI) MS methods are attractive because they do not require time-consuming chromatography, produce little to no chemical waste, and, thus, contribute to green chemistry practice. In addition, sample throughput can be higher compared to HPLC-MS. In this study, a method for the direct analysis of single- and multi-agent drugs using a plasma-based ADI source (flowing atmospheric-pressure afterglow, FAPA) coupled to high-resolution (HR) MS was developed and optimized for best performance. The approach is rapid and requires analytes to be in solution (only a few μL) before application onto thin-layer chromatography (TLC) surfaces, specifically dimethyl (RP2-) and cyano (CN-) modified silica, for surface-assisted (SA) FAPA-HRMS measurements. No chromatographic separation was required, and the TLC plates served only as sample carriers. A broad variety of 19 active pharmaceutical ingredients (APIs) was carefully selected to cover analgesics, anesthetics, antibiotics, antiepileptics, calcium channel blockers, diuretics, expectorants, opioids, peripheral vasodilators, stimulants, and sympathomimetics. Fast screening and identification of APIs were performed by SA-FAPA-HRMS. Typically, the protonated molecular ion ($[M + H]^+$) was the most abundant species, while some compounds (codeine, metamizole, phenoxymethylpenicillin, and torasemide) did show some degree of fragmentation. As a proof-of-principle application, benzocaine was directly detected in saliva samples post-intake of a lozenge. Time-resolved semi-quantitative screening was performed. The limit of detection for benzocaine in saliva was 8 ng mL^{-1} (48.4 fmol) using internal standard calibration and CN-HPTLC plates. In addition, direct quantification of artificially spiked saliva was performed with minimal sample preparation. Here, SA-FAPA-HRMS with a CN-HPTLC sample substrate yielded the best performance ($20.02 \pm 0.52 \mu\text{g mL}^{-1}$, RSD = 2.6%, and deviation of -1.9% from the theoretical value) compared to RP2-TLC ($18.97 \pm 1.37 \mu\text{g mL}^{-1}$ and RSD = 7.2%, -7.0%), and HPLC-UV ($18.51 \pm 0.03 \mu\text{g mL}^{-1}$ and RSD = 0.2%, -9.3%) results. In conclusion, SA-FAPA-HRMS is considered attractive for rapid and sustainable analysis of pharmaceuticals with potential in non-invasive patient monitoring.

Received 23rd June 2025
Accepted 2nd August 2025

DOI: 10.1039/d5ay01050k

rsc.li/methods

Introduction

Analytical sciences play an integral part in ensuring the safety and effectiveness of pharmaceuticals. For example, pharmacopoeias

strengthened purity testing, which has led to an increased use of high-performance liquid chromatography (HPLC) in quality control laboratories.¹ While HPLC systems with UV detectors were used early on, the invention of electrospray ionization (ESI)² led to the possibility of interfacing HPLC and mass spectrometry (MS),³ which, in turn, enabled structure identification, quantitation and impurity testing in complex samples. While powerful HPLC-MS methods for the characterization of different drug delivery systems exist, they share two limitations: (i) the requirement to use substantial amounts of solvents for sample preparation, analyte extraction/matrix removal (if applicable) and liquid

^aDepartment of Chemistry and Biology, University of Siegen, Adolf-Reichwein-Str. 2, 57076 Siegen, Germany. E-mail: carsten.engelhard@bam.de

^bResearch Center of Micro- and Nanochemistry and (Bio)Technology, University of Siegen, Adolf-Reichwein-Str. 2, 57076 Siegen, Germany

^cFederal Institute for Materials Research and Testing (BAM), Richard-Willstätter Str. 11, 12489 Berlin, Germany



chromatography, and (ii) they are very time-consuming because of the required steps mentioned before. Here, there is a need for faster, more sustainable, and environmentally friendly methods, which require less chemicals and produce less waste. A promising approach compared to classical chromatography-based methods is ambient desorption/ionization mass spectrometry (ADI-MS). While a very popular ADI source is solvent-based (desorption electrospray ionization, DESI)⁴ other methods operate solvent free and are laser- or plasma-based. One example of a plasma-based ADI source is DART (direct analysis in real time).^{4,5} DART-MS has been used for the identification of pharmaceuticals, detection of counterfeit drugs, and screening of drugs of abuse.^{6–9} Further applications were recently reviewed.^{10–13} In addition to DART, low-temperature plasma (LTP)-MS¹⁴ was used, for example, for the direct detection of active ingredients in Coartem (artemether and lumefantrine) and Malarone (atovaquone and proguanil hydrochloride) antimalarial tablets.¹⁵ A promising plasma-based alternative to DART and LTP is the flowing atmospheric-pressure afterglow (FAPA) probe coupled to MS, which was developed in the laboratories of G. M. Hieftje.^{16–18} After its introduction, the original pin-to-plate FAPA source geometry was further refined into a pin-to-capillary design that improved overall performance in terms of lower mass spectral background, reduced analyte oxidation and improved sensitivity.¹⁹ For improved sample introduction of solutions, vapors or aerosols, a so-called halo-FAPA source design was developed.²⁰

One common approach in ADI-MS is to probe dried residues of liquid samples from solid support materials readily available in the laboratory (microscope slides, stainless steel plates/mesh, and filter paper). In recent years, there has been interest in using thin-layer chromatography (TLC) plates as sample support materials. For example, TLC plates have been used with DART-MS,^{21,22} LTP-MS,²³ and DESI-MS^{24–28} for the analysis of a wide range of substances after planar separation. This included not only purely qualitative approaches but also quantitative detection of organophosphorus insecticides²² and semiquantitative imaging of biological extracts.²⁸ In addition, a so-called surface-assisted FAPA high-resolution MS (SA-FAPA-HRMS) method used TLC plates simply as sample substrates (without the need for a planar chromatography step) for the direct analysis of caffeine in beverages (energy drink, Coca-Cola, coffee, and black tea). Quantitation of caffeine in these beverages was performed by merely scanning the FAPA probe across the TLC plate and using co-deposited ¹³C₃-caffeine for internal calibration.²⁹ We have shown that a preceding planar chromatography step on a TLC plate can be beneficial in some FAPA-MS applications to remove matrix or potential interferences.^{29,30} Others have used a preceding planar chromatography step to remove the sample matrix, particularly when high-mass resolution was not available. For example, Ceglowski *et al.* used a combination of planar chromatography, low-cost laser ablation and FAPA ionization coupled to a quadrupole ion trap MS to characterize pyrazole derivatives, nicotine, sparteine, and an extract from a drug tablet (paracetamol, propyphenazone, and caffeine).³¹ In a series of studies, innovative techniques, including sheath-flow probe electrospray ionization (sfPESI)^{32,33} and paper spray ionization^{34–37} demonstrated advancements in

biofluid analysis and forensic applications using ambient mass spectrometry. Käser *et al.* reported advancements in online-breath analysis using secondary electrospray ionization-mass spectrometry (SESI-MS) for the detection of endogenous compounds in exhaled breath.³⁸ Additionally, dielectric barrier discharge ionization mass spectrometry enabled direct analysis of fentanyl analogs in blood and plasma samples.³⁹ Further applications of ADI-MS including analysis of drugs and toxins were recently reviewed by Henderson *et al.*⁴⁰

In this work, we present a proof-of-principle study for the direct characterization of a broad variety of active pharmaceutical ingredients (APIs) in over-the-counter and prescription drugs using functionalized thin-layer surfaces (without the need for a planar chromatography step) and plasma-based desorption/ionization coupled to high-resolution mass spectrometry (HRMS). To also demonstrate direct and non-invasive drug monitoring possibilities, a semiquantitative and time-resolved screening for benzocaine was performed using saliva. Benzocaine was selected because it is freely available to consumers and is often used during the cold season, and because saliva sample collection is rapid and non-invasive. Sample preparation and the use of solvents and chemicals was kept to a minimum across all investigations. SA-FAPA-HRMS results were compared to and validated by HPLC.

Materials and methods

Reagents

Methanol (HPLC grade) was purchased from Fisher Chemicals (Hampton, NH, USA). Benzocaine (98% chemical purity) was obtained from Acros Organics (Geel, Belgium) and *D*₄-benzocaine (chemical purity 98%, isotopic purity 99.9%) was obtained from Toronto Research Chemicals (Toronto, Canada). Other active pharmaceutical ingredients (APIs) were purchased from pharmacies. The most important information on the APIs is summarized in Table 1.

Preparation of standard solutions

The preparation of API standard solutions was kept to a minimum. Drug capsules were weighed and ground before dissolving a small amount (1.4–10.4 mg) in methanol (1–10 mL depending on API content). After 15 minutes of ultrasonic treatment, solutions were microfiltered (0.45 μm) to eliminate insoluble filler materials. The concentrations related to the active ingredient content of each capsule are presented in Table 1. In addition, a standard solution series with analytically pure benzocaine was prepared, ranging from 10 ng mL⁻¹ to 100 μg mL⁻¹. For HPLC validation experiments, two sets of benzocaine standards were prepared (see the SI for details). A methanolic internal standard (IS) solution was prepared containing 1 μg mL⁻¹ *D*₄-benzocaine. Table 2 summarizes the achieved performance parameters of SA-FAPA-MS for benzocaine analysis.

Preparation of saliva samples

This study involved the collection of saliva samples from a healthy volunteer and was performed following the principles



Table 1 Information on the APIs included in this study. Quantitative data for the tablets are based on the information given on the drug packaging

API	Drug name	Brand	m% _{API} in capsule ^a	<i>m</i> _{weighed} [mg]	<i>V</i> _{MeOH} [mL]	<i>C</i> _{API} [μg mL ⁻¹]
Acetaminophen	Oxycodone-APAP	CVS/Pharmacy	61.4	8.1	3.0	1658
	Migraene-Kranit®	Krewel Meuselbach	33.2	9.1	1.0	3021
Ambroxol	Mucosolvan®	Sanofi	34.6	1.8	2.0	311.4
Amlodipine	Amlodipin	Dexcel® Pharma	2.5	5.3	2.0	66.2
Aspirin	Aspirin® complex	Bayer	18.2	7.0	10	127.4
	Dolviran®	Bayer	31.5	10.4	1.0	3276
Benzocaine ^b	Dolo-Dobendan®	Reckitt Benckiser	0.4	—	—	—
Caffeine	Migraene-Kranit®	Krewel Meuselbach	14.1	9.1	1.0	1283
	Dolviran®	Bayer	7.9	10.4	1.0	821.6
Codeine	Dolviran®	Bayer	1.5	10.4	1.0	156.0
Diclofenac	Diclo KD® 75 akut	DR. KADE	31.4	3.8	1.0	1193
Doxycycline	Doxycyclin 100	1A Pharma	51.4	1.8	2.0	462.6
Ethaverine	Migraene-Kranit®	Krewel Meuselbach	3.3	9.1	1.0	300.3
Ibuprofen	IBU 600	1A Pharma	84.0	2.1	2.0	882.0
Metamizol	Novaminsulfon	Zentiva	76.5	2.8	2.0	1071
Naproxene	Naproxene	CVS/Pharmacy	95.5	2.7	3.0	859.5
Oxycodone	Oxycodone-APAP	CVS/Pharmacy	0.9	8.1	3.0	24.3
Phenacetin	Dolviran®	Bayer	31.5	10.4	1.0	3276
Phenobarbital	Migraene-Kranit®	Krewel Meuselbach	5.0	9.1	1.0	455.0
	Dolviran®	Bayer	3.9	10.4	1.0	405.6
Penicillin V	Pen 1,5 Mega	1A Pharma	86.5	1.4	2.0	605.5
Propyphenazone	Migraene-Kranit®	Krewel Meuselbach	24.9	9.1	1.0	2266
Pseudoephedrin	Aspirin® complex	Bayer	1.1	7.0	10	7.7
Torsemide	Torsemid	1A Pharma	6.2	6.5	2.0	201.5

^a Mass percent based on information from the drug packaging. ^b Consumed as Dolo-Dobendan® (Reckitt Benckiser) as a whole lozenge and probed from saliva samples.

Table 2 Performance parameters of the SA-FAPA-MS methods for benzocaine analysis using either RP2-TLC or CN-HPTLC as the sample carrier surface with or without including an internal standard

Sample carrier surface	<i>R</i> ²	LOD [ng mL ⁻¹]	LOQ [ng mL ⁻¹]
No internal standard used ^a			
RP2-TLC	0.9914	13	42
CN-HPTLC	0.9965	12	40
Internal standard used ^b			
RP2-TLC	0.9996	11	38
CN-HPTLC	0.9978	8	28

^a Performance parameters based on calibration using 10 ng mL⁻¹–100 μg mL⁻¹ benzocaine standards. ^b Performance parameters based on calibration using 10 ng mL⁻¹–100 μg mL⁻¹ standards, each spiked with a *D*₄-Benzocaine standard (1 μg mL⁻¹).

of the Helsinki Declaration. It was approved by the Ethics Committee of the University of Siegen, Germany, under reference number LS_ER_22_2025. First, blank saliva before API intake was collected using Salivette sample tubes (SARSTEDT AG & Co., Nümbrecht, Germany). To collect trapped saliva from the cotton sponge, the sample tube was centrifuged at a speed of 3200 rpm (revolutions per minute) for two minutes using an EBA 20 centrifuge (Andreas Hettlich GmbH & Co. KG, Tuttingen, Germany). The saliva was stored at –18 °C until use to avoid changes in composition due to aging processes.

Samples for the benzocaine screening experiments were collected from a healthy volunteer immediately after

consumption of a lozenge and at 10 min intervals for a total of 120 min after consumption (total of 13 samples). On days when saliva samples were collected, only water and caffeine-free tea were consumed, and sampling was performed only before large meals to minimize interferences.

HPTLC preparation

Glass-backed TLC plates (3.3 cm × 3.3 cm, cut from 10 cm × 20 cm standard plates, CN-HPTLC and RP2-TLC, both MACHEREY-NAGEL, Düren, Germany) were used as sample carriers. A Linomat V spray-on application system (CAMAG, Muttenz, Switzerland) was used for sample deposition at a dosing speed of 50 nL s⁻¹. The spraying distance was set to 2.4 mm between the syringe tip and sample carrier surface. The step size (distance between different sample spots) was kept constant at 5 mm. Samples were analyzed in triplicate, *i.e.*, three 1 μL aliquots were sprayed onto the plates in proximity. It is important to note that no time-consuming drying step was required and no chromatographic step was performed.

Instrumentation

For mass spectrometric analysis, an Exactive HCD Orbitrap (Thermo Fisher Scientific, Bremen, Germany) was coupled to a home-built pin-to-capillary FAPA ionization source. The mass spectrometer was calibrated weekly with a conventional ESI source. For positive ion mode calibration, the Pierce® LTQ ESI positive ion calibration solution (Thermo Fisher Scientific, Bremen, Germany) with caffeine (20 μg mL⁻¹), Met-Arg-Phe-Ala



(MRFA, $1 \mu\text{g mL}^{-1}$) and Ultramark 1621 (0.001%) in an aqueous solution of acetonitrile (50%), methanol (25%) and acetic acid (1%) was used. For negative ion mode calibration, the Pierce® LTQ ESI negative ion calibration solution (Thermo Fisher Scientific, Bremen, Germany) was used. Instead of caffeine and MRFA, the solution contained sodium dodecyl sulfate ($2.9 \mu\text{g mL}^{-1}$) and sodium taurocholate ($5.4 \mu\text{g mL}^{-1}$). The mass resolution was set to 50 000 (at 200 m/z). The day-to-day mass measurement uncertainty did not exceed 2 ppm in the positive ion mode and 4 ppm in the negative ion mode. To ensure high mass accuracy, positive ion mode measurements included lock masses of ubiquitous species (phthalic anhydride fragment at 149.2033 m/z ; *n*-butylbenzenesulfonamide at 214.0896 m/z). In negative ion mode, no comparable species were detectable at sufficient abundance.

The FAPA ionization source discharge chamber consisted of Macor® ceramic (Schröder Spezialglas, Ellerau, Germany). A stainless-steel pin cathode (1.6 mm outer diameter (o.d.), 100 mm length, sharpened tip) and a capillary-anode (1.6 mm o.d., 1.0 mm inner diameter (i.d.), 15 mm length) were screwed into the discharge chamber. The cathode-to-anode distance was 7.5 mm. To generate the helium discharge, a negative potential was applied to the cathode through a 5 k Ω resistor, and a DC power supply (Kepco, Flushing, NY, USA) was operated in current-controlled mode at a helium flow rate of 750 mL min^{-1} using grade 5 helium (Messer Industriegase GmbH, Siegen, Germany). At 25 mA, the resulting potential was around 650 V. For mounting the FAPA source on the MS, a bracket with a suitable connection that matches the conventional ESI source bracket on the instrument inlet was used. A motorized stage (Newport Corporation, Irvine, CA, USA) integrated into the mounting device positioned the sampling surfaces beneath a curved ion transfer capillary (0.6 mm inner diameter, 40 mm extension). The stage was controlled with a custom LabVIEW (Version 11.0, 2011, National Instruments, Austin, TX, USA) program. For mass spectrometric experiments, an angle of 70° and a distance of 1.0 mm between the FAPA outlet capillary and the respective desorption surface was set. The distance between the surface and ion transfer capillary was adjusted to 0.5 mm and the distance between the ion transfer capillary and FAPA outlet capillary was maintained at 1.0 mm. TLC plates were fixed on the motorized stage using a spring-loaded clamp.

Molecular mapping and data analysis

Two-dimensional (2D) molecular maps were generated by linear scanning of the TLC surface at a scanning speed of 0.3 mm s^{-1} in the *x*-direction with a line spacing of 0.5 mm in the *y*-direction. The LabVIEW program that was used to control the stage motion was also used to trigger the data acquisition for automated MS imaging. Individual *x*-line scans were summed to form 2-dimensional molecular maps by converting the time for one line scan into distance based on a scan rate of 0.3 mm s^{-1} . The *y*-axis distance was determined by the total number of lines acquired at 0.5 mm intervals. These parameters, combined with XIC abundances, were used to generate contour plots. In the contour plots, the so-called regions-of-interest (ROIs) were used

and integrated, to gain abundance information for the individual APIs.

Exactive Tune software (Version 1.1 SP6, Thermo Scientific, Bremen, Germany) was used to control the MS and to acquire data. Analyte-selective information was acquired from extracted ion chromatograms (XICs) within a m/z -range of ± 4 ppm in positive ion mode according to Table S1 and within a m/z -range of ± 6 ppm in negative ion mode according to Table S2. The differences were chosen based on instrumental variations in the two ion modes. Further data processing was performed with MZmine 2.53 and Origin 2017 (OriginLab Corporation, Northampton, MA, USA).

Safety considerations

The experimental setup used for the experiments involved potentially harmful voltages and currents to operate the FAPA source. Connections between the power supply and the ionization source were insulated to prevent potential electric shocks. An acrylic enclosure was used to cover the FAPA source to prevent vaporized solvents and potentially toxic or corrosive chemicals and by-products from entering the laboratory atmosphere and to protect the experimental setup from contamination and interferences.

Results and discussion

Direct analysis of single-agent drugs on cyano and dimethyl surfaces using FAPA-MS

Drug preparations can be classified into two groups depending on the number of active ingredients combined in one tablet. Monopreparations are pharmaceutical compositions that contain a matrix and only one active ingredient. When two or more active ingredients are combined (*e.g.*, in a tablet) this approach is called a combination preparation or combination drug. Fast qualitative screening of pharmaceutical preparations with a straightforward MS procedure is desirable not only for quality assurance. In the first part of this study, the feasibility of direct and fast monopreparation analysis using SA-FAPA-MS was studied (monopreparations are referred to as single-agent drugs throughout the text). For direct analysis, single-agent drugs were simply applied onto carefully selected TLC surfaces as sample substrates. These sample substrates have advantages over conventional substrates such as glass or metal as reported earlier.^{29,41} For example, improved reproducibility and reduced analyte diffusion were reported, which are critical for accurate quantitative results. The selection of surface modification and solvent (methanol) in this study was based on previously published data demonstrating the excellent properties of CN- and RP2-modified surfaces for direct desorption/ionization mass spectrometry of small molecules.⁴¹

Fig. 1A shows a direct comparison of the ion abundance of nine different APIs (see Table S1 for information on specific m/z) when probed with FAPA-MS directly from CN-HPTLC (green) and RP2-TLC (yellow) surfaces. Please note that no preceding planar chromatography step was applied. As a general observation it was found that the use of RP2-TLC for the APIs



investigated in this study was beneficial over CN-HPTLC plates because the signals were mostly comparable or higher than those from RP2-TLC. The largest signal increase (from CN-HPTLC to RP2-TLC) was recorded for ambroxol ($[M + H]^+$, m/z_{theo} 378.9838 for $^{79}\text{Br}^{81}\text{Br}$ -species, positive ion mode). This observation is consistent with a previous study, in which the use of RP2 surfaces was also found to be beneficial although for a different set of compounds (caffeine, acetaminophen, progesterone, and nicotine).⁴¹ In Fig. 1B and C, the APIs are ordered by the absolute amount of active ingredient applied onto the surface in nmol. For almost all compounds, a correlation between the amount applied on the surface and the

resulting ion abundance after FAPA-MS analysis can be observed. Typically, in positive ion mode the protonated species ($[M + H]^+$) of the APIs were the most abundant species compared to, e.g., fragment ions. A slightly higher degree of fragmentation or adduct formation was observed for amlodipine, codeine, ibuprofen, metamizole, and phenoxymethylpenicillin. Specifically, the protonated species were not the predominant ions in the mass spectra (see Table S1 for detailed information). Among the studied compounds, doxycycline ($[M + H]^+$, m/z_{theo} 444.1527, positive ion mode) was found to be an exception. This compound exhibited the lowest ion abundance in FAPA-MS for both TLC surfaces even though three other compounds

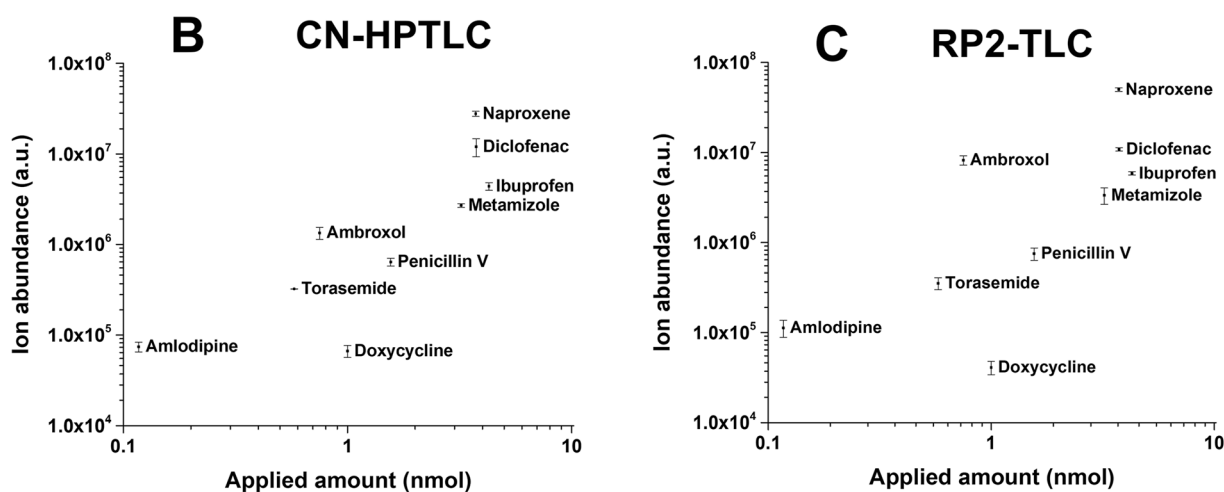
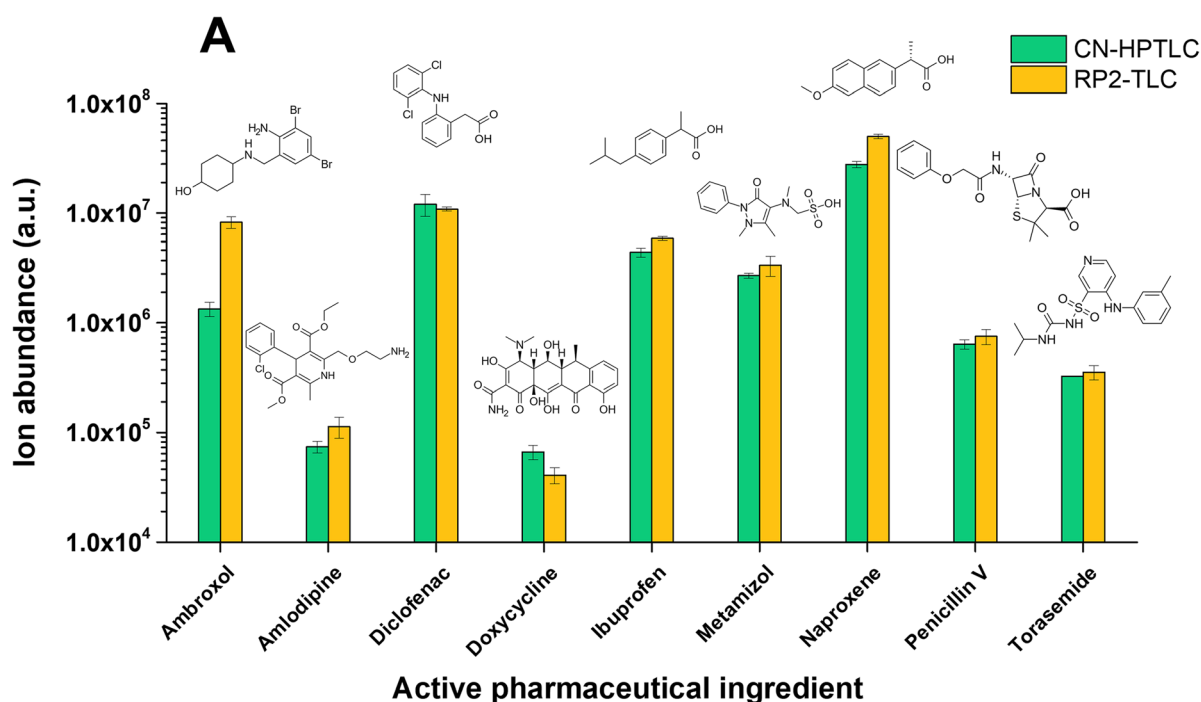


Fig. 1 Direct API screening of single-agent drugs in tablets using SA-FAPA-HRMS and minimal sample preparation: influence of sample substrates on ion abundance of nine APIs probed from CN-HPTLC (A, in green) and RP2-TLC (A, in yellow) surfaces without a preceding planar chromatography step. Overview of ion abundance vs. applied API amount (depending on the commercialized drug content dissolved in MeOH) after analyte desorption/ionization from CN-HPTLC (B) and RP2-TLC (C). Error bars correspond to $n = 3$ replicates and represent the standard deviation. Note the logarithmic scaling. Signals are integrated molecular contour plots of analyte species according to Table S1.



including amlodipine ($[M-C_3H_8NO]^+$, m/z_{theo} 334.0841 for ^{35}Cl -species, positive ion mode) were probed at a lower nominal concentration (1 nmol of applied doxycycline vs. 0.117 nmol of applied amlodipine). Given the different structures and properties of the compounds mentioned above, a difference in ion abundance would not be surprising. Clearly, such comparisons should be interpreted with caution because the recorded ion signals result from a combination of factors (desorption/ionization efficiency, degree of fragmentation, ion transmission, *etc.*). To further investigate the desorption and ionization behavior of doxycycline, comparative experiments with tetracycline were performed. This pair was selected because doxycycline and tetracycline are structural isomers that differ only at one hydroxyl substitution site (-3,5,10,12,12a-pentahydroxy- vs. -3,6,10,12,12a-pentahydroxy-). While the signal of doxycycline was already small compared to other APIs, tetracycline was not detectable at all in positive ion mode (data not shown). A similar trend was observed in negative ion mode (see Fig. 4 in the section “Comparison of positive and negative ion mode” for selected APIs.) While it is not the aim of the present study to investigate the influence of molecular differences on the desorption and/or ionization efficiency in ADI-MS in detail, this example illustrates possible effects of small molecular differences. Clearly, quantitative FAPA-MS methods will benefit from internal and matrix-matched standardization.

Analysis of multi-agent drugs on cyano and dimethyl surfaces

Multi-agent or combination drugs contain two or more active ingredients and are often prescribed. A significant advantage is the reduced pill burden for patients making it easier to manage medication intake and thus reduce adverse side effects.⁴² In the second part of the study, several multi-agent drugs, namely Aspirin® complex, Dolviran®, Migraene-Kranit®, and Oxycodone-APAP (Table 1) were probed by SA-FAPA-HRMS. The

inclusion of multi-agent drugs provides an opportunity to investigate the competitive behavior of different compounds with each other in terms of desorption and ionization efficiency. This so-called competitive ionization can be a challenge in ADI-MS and has been reported, for example, for multi-analyte standards in a previous FAPA-MS study.⁴¹ It was shown that the presence of high nicotine concentrations led to significant signal losses for other simultaneously present analytes (*e.g.*, progesterone).

For this study, two multi-agent drugs were probed that contain two APIs (and matrix), namely Aspirin® Complex and Oxycodone-APAP. SA-FAPA-HRMS results are summarized in Fig. 2 and S1.

In the multi-agent drugs, both aspirin (0.707 nmol) and acetaminophen (10.96 nmol) are present in significantly larger amounts compared to pseudoephedrine (0.038 nmol) and oxycodone (0.069 nmol), respectively. When comparing the applied amounts of aspirin and pseudoephedrine to their corresponding mass spectral signals (see Fig. 2), it can be concluded that the use of RP2 surfaces is more favorable than CN-HPTLC. While significantly more aspirin, referred to as the excess factor throughout the text (~20-fold more deposited aspirin compared to pseudoephedrine), was applied to both TLC surfaces, an approximately 3300-fold higher signal for aspirin compared to pseudoephedrine was recorded when the FAPA source probed the CN surface. In contrast, the aspirin signal was approximately 520-fold higher using RP2-TLC plates as the sample substrate. A consistent trend is observed for oxycodone APAP. Here, the excess factor is approximately 159 for administered acetaminophen compared to oxycodone. The signal on the CN surface is 630-fold higher for acetaminophen compared to oxycodone. On the RP2 surface, a 210-fold higher signal was measured for acetaminophen, which is quite close to the respective excess factor. In general, stronger analyte signals

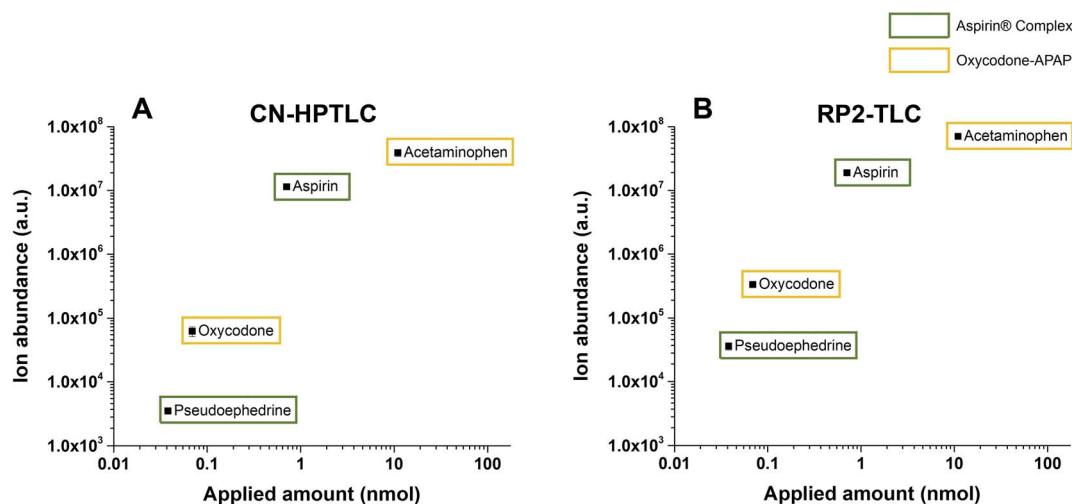


Fig. 2 Direct API screening of multi-agent drugs in tablets using SA-FAPA-HRMS and minimal sample preparation: overview of ion abundance vs. applied API amount (depending on the commercialized drug content dissolved in MeOH) after analyte desorption/ionization from CN-HPTLC (A) and RP2 TLC (B). Highlighted in green are the APIs in Aspirin® Complex (aspirin and pseudoephedrine) and highlighted in yellow are the APIs in Oxycodone-APAP (oxycodone and acetaminophen). Error bars correspond to $n = 3$ replicates and represent the standard deviation. Note the logarithmic scaling. Signals are integrated molecular contour plots of analyte species according to Table S1.



were obtained using RP2 surfaces compared to those obtained using CN-HPTLC plates, which is consistent with our previous results.⁴¹

After screening the multi-agent drugs with two APIs, more complex multi-agent drugs with five APIs, namely Dolviran® and Migraene-Kranit®, were studied with FAPA-MS. Information on the compounds and detected ions is given in Tables 1 and S1. In Fig. 3, analyte ion responses of the APIs in Dolviran® and Migraene-Kranit® are summarized for two different surfaces. Unlike single-agent drugs (Fig. 1), a mixture of compounds was presented to the desorption/ionization source. Here, matrix effects due to *e.g.*, competitive ionization or preferential desorption effects could potentially influence the results. These effects typically become more pronounced with increasing analyte concentration and/or matrix and fundamental parameters such as proton affinity (PA) and enthalpy of vaporization (ΔH_{vap}) are important to consider.⁴¹ When

comparing the two molecules present at the highest amounts in Dolviran®, namely aspirin (18.18 nmol applied) and phenacetin (18.28 nmol applied), ion abundance differences are readily recognizable (Fig. 3A and B). The phenacetin signal is approximately 8-fold higher with CN-HPTLC and 19-fold higher with RP2-TLC compared to aspirin even though the nominal concentrations in the drug formulation are very similar. This signal difference is assumed to be a result of the different physicochemical properties of the molecules. Phenacetin is a 4-substituted acetanilide derivative and shows structural similarities to acetaminophen (difference is the 4-ethoxy group compared to the 4-hydroxy group in acetaminophen).

Because no reliable PA values for phenacetin were found in the literature, acetaminophen was used to estimate the PA value (because the protonation sites remain almost the same). The PA values for the most favored protonation sites in acetaminophen range from 887 to 915 kJ mol⁻¹.⁴³ For aspirin, the PA for the

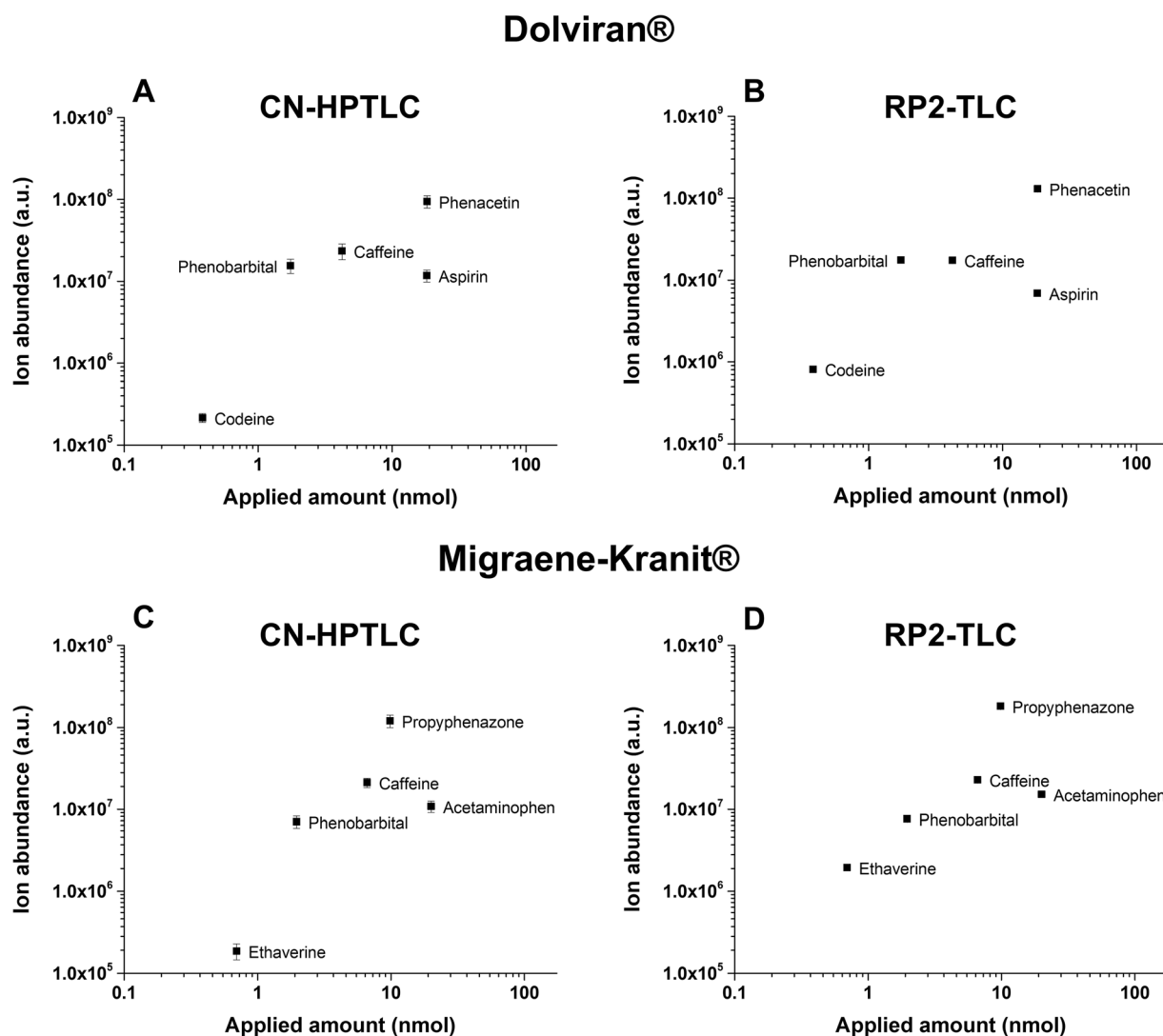


Fig. 3 Direct API screening of multi-agent drugs in tablets using SA-FAPA-HRMS and minimal sample preparation: overview of ion abundance vs. applied API amount (depending on the commercialized drug content dissolved in MeOH) for Dolviran® (upper section) after analyte desorption/ionization from CN-HPTLC (A) and RP2-TLC (B) and for Migraene-Kranit® (lower section) after analyte desorption/ionization from CN-HPTLC (C) and RP2-TLC (D). Error bars correspond to $n = 3$ replicates and represent the standard deviation. Note the logarithmic scaling. Signals are integrated molecular contour plots of analyte species according to Table S1.



most preferred site of protonation, precisely the carbonyl oxygen of the carboxylic acid group, was obtained through density functional theory (DFT) calculations and found to be $867.8 \text{ kJ mol}^{-1}$.⁴⁴ If one assumes that the PAs of acetaminophen can serve as an approximation for phenacetin, the latter is expected to have a higher PA compared to aspirin. This, in turn, would result in preferential proton transfer ionization of phenacetin in the presence of aspirin. In fact, mass spectra of the multi-agent drug did reveal that the most abundant ion species of phenacetin was in fact the protonated $[M + H]^+$ molecular ion. Aspirin on the other hand underwent deacetylation and was mainly detected as the $[M-C_2H_3O_2]^+$ -species. This deacetylation may also be induced by prior protonation; however, this protonation site was not mentioned in the DFT simulations.

Another API in Dolviran® is caffeine (4.23 nmol applied, 3rd highest nominal concentration in the drug formulation), which was detected as the protonated molecular ion ($[M + H]^+$) and little fragmentation. Compared to caffeine, the amount of phenacetin applied to the surface was 4.3 times higher. This corresponds approximately to the measured difference in ion abundance, which was about 4.0 times higher for phenacetin compared to caffeine. All other APIs in the drug were successfully detected as well.

In the second multi-agent drug Migraene-Kranit®, acetaminophen (19.99 nmol applied) and propyphenazone (9.84 nmol applied) were the APIs with the highest nominal concentration. Although the applied amount of acetaminophen was more than twice that of propyphenazone, acetaminophen exhibited significantly lower ion abundance on both surfaces (Fig. 3C and D: 11-fold lower with CN and 12-fold lower with RP2 plates). For both molecules the $[M + H]^+$ -species was the most abundant ion in the mass spectrum. Although PA values for acetaminophen are available for its favored protonation sites (887 to 915 kJ mol^{-1}) we could not find literature data for the PA of propyphenazone itself. The basic structure of propyphenazone is a heteroaromatic pyrazole, or more precisely a pyrazolone. The CRC Handbook of Chemistry and Physics gives an overview of the PAs of various pyrazole derivatives.⁴⁵ Comparing the different derivatives, it is evident that the PA increases with increasing alkyl or phenyl substitution (Table S3). For instance, the dialkyl and diphenyl derivatives of pyrazole show significantly higher PAs (927.3 – $946.3 \text{ kJ mol}^{-1}$) than the unsubstituted pyrazole ($894.1 \text{ kJ mol}^{-1}$).⁴⁵ It was therefore assumed that propyphenazone would have a higher PA compared to acetaminophen. This, in turn, would lead to more efficient proton transfer ionization of propyphenazone compared to acetaminophen, which is in agreement with the observed ion abundances of the protonated molecular ions in this work.

In terms of the two different TLC surfaces, only minor differences in ion abundances were observed. Overall, RP2-TLC plates showed slightly better performance for the APIs at higher concentrations and were really helpful for detecting compounds at lower amounts (except for phenobarbital). For ethaverine, codeine, pseudoephedrine and oxycodone, ion abundances were found to differ significantly depending on the surface

used. Sensitivity for these compounds was higher when they were applied onto and desorbed from RP2-functionalized surfaces. This finding is in good agreement with previous results for acetaminophen and progesterone on RP2-TLC.⁴¹

Comparison of positive and negative ion mode

Previous studies on surface-assisted FAPA-MS focused mainly on positive ion mode detection. The molecular variety and different functionalities of the APIs included in this study, however, gave an opportunity to compare the performance of the method in both positive and negative ion mode. For this comparative study, APIs were selected that are either present as alkali salts or feature a carboxyl group. Fig. 4 compares the FAPA-HRMS results in positive and negative ion modes for both TLC types. Some differences are evident, although less clearly pronounced than initially expected. For metamizole and naproxene, the detection in positive ion mode yielded significantly higher analyte signals independent of the desorption surface. Diclofenac detection in positive ion mode was beneficial with a higher signal observed when the CN-HPTLC sample substrate was used. Penicillin V detection in negative ion mode after deposition on CN-HPTLC surfaces did show a better performance compared to RP2-TLC. In contrast, the Penicillin V signal was higher in positive ion mode when the RP2 surface is used. While a detailed mechanistic study is beyond the scope of this study, it would be an interesting topic for future investigation. In future applications, both detection modes should be carefully evaluated during method optimization for best performance.

Direct (semi-)quantitative benzocaine screening from saliva samples

The use of drugs necessitates diagnostic analysis, especially in clinical trials and for patient monitoring and safety. This usually includes bio fluids such as whole blood, serum, plasma, and urine as well as sweat or saliva. The latter offer the advantage of non-invasive sampling, which is gentle for patients and particularly attractive in pediatrics. The so-called Salivettes have become established tools for collecting saliva samples. Here, a cotton sponge is used to absorb salivary fluid, which is then collected by centrifugation. In terms of a proof-of-principle study, SA-FAPA-HRMS was tested for time-resolved saliva screening to semiquantitatively monitor salivary benzocaine. Saliva samples were collected over a defined period after consumption of a lozenge containing the active ingredient which is available over the counter. The samples were analyzed directly in 10-minute increments without further preparation. Fig. 5 illustrates the workflow and representative results over a 70-minute period.

The benzocaine signal decayed and reached its minimum after 70 min which corresponds to eight saliva samples that are included. In the five remaining samples (80–120 min after consumption), no benzocaine was detectable.

For better interpretation of these semiquantitative data, it is important to consider the performance parameters of the corresponding SA-FAPA-HRMS method. Table 2 compares the



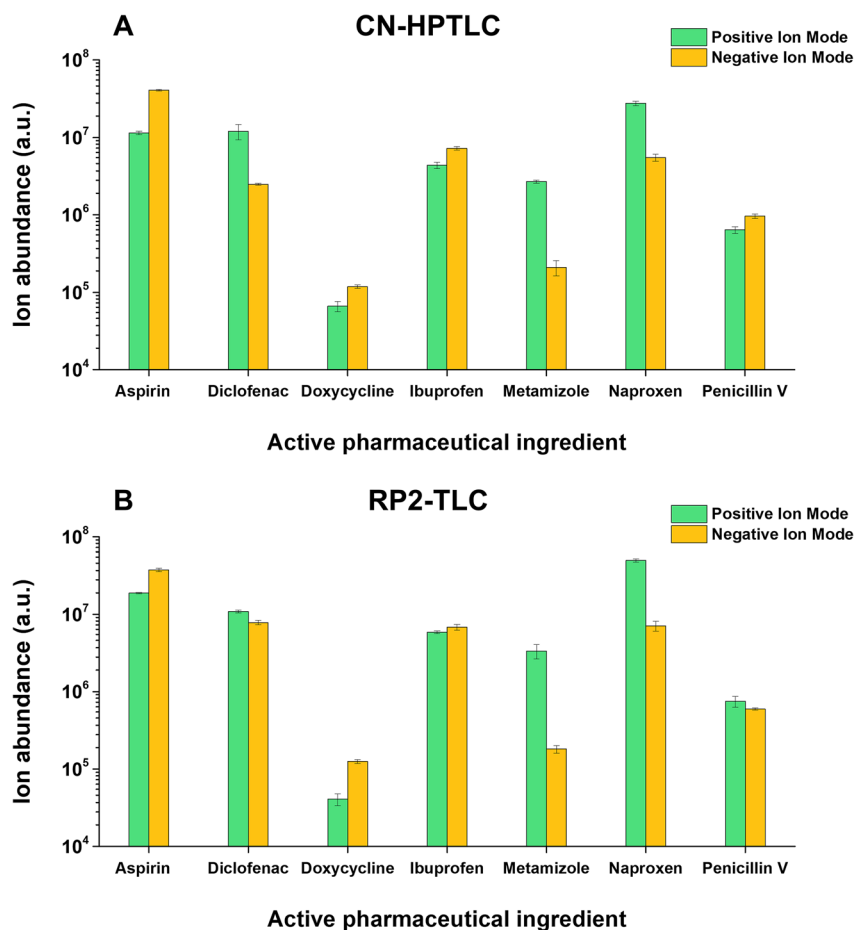


Fig. 4 Ion abundances of selected APIs in positive (green) and negative (yellow) ion modes based on desorption and ionization from CN-HPTLC (A) and RP2-TLC (B). Error bars correspond to $n = 3$ replicates and represent the standard deviation. Note the logarithmic scaling.

respective parameters using RP2-TLC or CN-HPTLC as the sample substrate either with or without the use of an IS. The use of CN-modified surfaces achieved slightly better limits of detection (LODs) and limits of quantification (LOQs), as did the use of an IS. Hence, the best sensitivity was obtained by internal standardization and desorption from CN-HPTLC surfaces with

an LOD of 8 ng mL^{-1} . The best achievable LOD using RP2-TLC was 11 ng mL^{-1} . With respect to the results shown in Fig. 5 based on desorption from RP2-TLC without using an IS, the lowest salivary benzocaine concentration at 70 min after lozenge consumption can be estimated to be slightly higher than 13 ng mL^{-1} . For comparison of the semi-quantitative

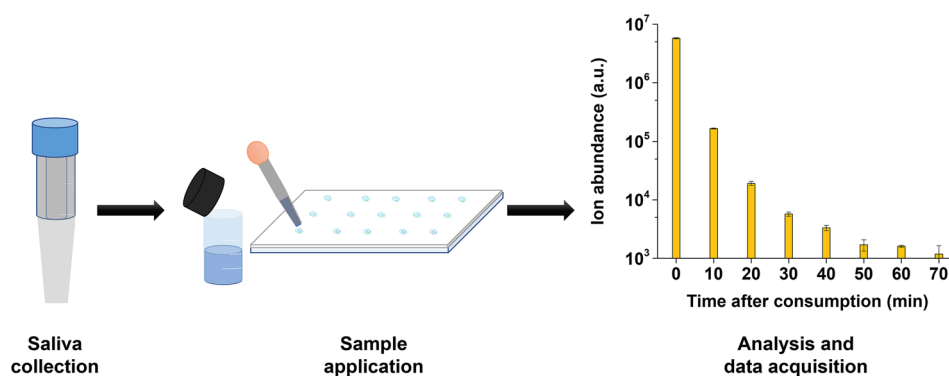


Fig. 5 Workflow of the non-invasive, semiquantitative benzocaine screening in saliva samples. The samples are collected via Salivettes and centrifuged. After application of $1 \mu\text{L}$ of untreated saliva per spot ($n = 3$ per time increment) the RP2 surface is analyzed by SA-FAPA-MS and the data are further evaluated. Error bars correspond to $n = 3$ replicates and represent the standard deviation. Note the logarithmic scaling in the right graph.



findings with quantitative results, the saliva samples were also analyzed by HPLC-MS using internal standard calibration (SI). Here, benzocaine in the first saliva sample (0 min) was very high (approximately $36.5 \mu\text{g mL}^{-1}$) and out of the calibration range (10 ng mL^{-1} – 100 ng mL^{-1}) of the method. Nevertheless, the rapid benzocaine decrease in saliva could be monitored all the way to falling below the LOD after 60 min post-intake. The HPLC-MS method R^2 was 0.9973 and the achieved LOD was 6.1 ng mL^{-1} . Starting at 60 min post-intake and later, signals were below the LOQ and LOD determined for the HPLC-MS method. As the method does not offer any separation options, interference cannot be ruled out. These can be caused by the body's own molecules or metabolic products as well as by isobaric environmental substances. In multi-drug agents, different active substances can also be degraded into the same metabolites, which can also lead to interferences and misinterpretations during detection and data analysis. Especially with regard to clinical applications, this must be taken into account for accurate data interpretation.

For direct accurate benzocaine quantification in saliva samples with SA-FAPA-MS, an artificial saliva sample with a known benzocaine amount ($20.4 \mu\text{g mL}^{-1}$) was prepared and analyzed using an IS calibration approach including four standards (SI). Based on CN-HPTLC as the sampling substrate, a calibration curve with an R^2 of 0.9922 was obtained. Further calculation of the benzocaine content in the salivary sample resulted in a concentration of $20.02 \pm 0.52 \mu\text{g mL}^{-1}$. This corresponds to a small deviation of -1.9% from the theoretical value of $20.4 \mu\text{g mL}^{-1}$. Additionally, the same procedure was performed using RP2-TLC as the sampling substrate. Here, an R^2 of 0.9949 was achieved and the calculated concentration was $18.97 \pm 1.37 \mu\text{g mL}^{-1}$, which corresponds to a deviation of -7.0% from the theoretical value. For validation purposes, a HPLC-UV method was also used (SI) on the same artificially prepared saliva sample using external standard calibration. Here, a benzocaine concentration of $18.51 \pm 0.03 \mu\text{g mL}^{-1}$ was determined (deviation of -9.3% from the theoretical value). When comparing the SA-FAPA-MS results with the HPLC-UV validation results, deviations of $+8.2\%$ for CN-HPTLC based analysis and $+2.5\%$ for RP2-TLC based analysis were achieved.

As shown above both the semiquantitative and the fully quantitative approach can yield results for the direct analysis of benzocaine in untreated saliva samples that are in good agreement with those obtained from standard HPLC methods. We believe that these promising results make FAPA-HRMS an attractive tool for fast API screening, especially due to the non-invasive nature of collecting patient samples when using saliva. This method is particularly suitable for orally applied drugs, other biofluids could also be analyzed, which can significantly increase the range of possible analytes.

Conclusion

SA-FAPA-HR-MS has been successfully applied to the direct analysis of pharmaceutical products. As a solvent-free and rapid screening method, it can be a promising addition to the toolbox for pharmaceutical analysis. API detection was successfully

demonstrated for single-agent drugs and multi-agent drugs. This is particularly advantageous for the latter because no extraction or separation steps were required, and all APIs could be detected simultaneously (provided that no isomers are present). Furthermore, minimum amounts of liquid sample solution ($1 \mu\text{L}$) were required. Simultaneous API detection in multi-agent drugs, even with significant concentration differences within a tablet, is feasible using surface-assisted desorption/ionization. This method proves effective over a broad dynamic range and efficiently detects a variety of drug molecules, with the choice of negative or positive ion mode having little impact on results, rendering it a practical and reliable routine approach.

Sensitivity was demonstrated using benzocaine detectable at low ng mL^{-1} (ppb), corresponding to low fmol amounts, highlighting the suitability of the method for diagnostic applications. It was successfully employed to track benzocaine levels in saliva after oral administration, enabling semi-quantitative monitoring of its decrease over a defined time frame. Calibration-based quantification in an artificial sample showed its promising diagnostic potential with minimal, non-invasive efforts, including validation against established methods like HPLC-UV.

SA-FAPA-MS holds promise as a rapid mass spectrometry technique for drug analysis and direct diagnostics. Its potential extends beyond saliva to other biofluids, and it may also find applications in kinetic studies for reaction control in the future.

Compliance with ethical standards

The manuscript was written with contributions from all authors. All authors have given approval to the final version of the manuscript. The reference number of the Institutional Ethics Board for this study is LS_ER_22_2025.

Conflicts of interest

There are no conflicts to declare.

Data availability

Supporting data are partially included in the SI. Additional data that support the findings of the saliva study are available from the corresponding author upon reasonable request. Participants of this study did not give written consent for their data to be shared publicly.

Supplementary information: Detailed mass spectrometric parameters of investigated APIs, FAPA-MS analysis of multi-agent drugs, proton affinity data of pyrazole derivatives, and HPLC-based validation of benzocaine concentrations in saliva. See DOI: <https://doi.org/10.1039/d5ay01050k>.

Acknowledgements

The authors thank MACHEREY-NAGEL, Düren, Germany, for helpful discussions. All members of the mechanical workshop in the Department of Chemistry and Biology at the University of



Siegen are gratefully acknowledged for their support, manufacturing of custom parts, and help with instrument maintenance. Special thanks go to Bernd Meyer and Markus Rabe.

References

- World Health Organization, *WHO good practices for pharmaceutical quality control laboratories*, TRS, 2010, vol. 957, pp. 81–129.
- M. Yamashita and J. B. Fenn, *J. Phys. Chem.*, 1984, **88**, 4451–4459.
- C. M. Whitehouse, R. N. Dreyer, M. Yamashita and J. B. Fenn, *Anal. Chem.*, 1985, **57**, 675–679.
- Z. Takats, J. M. Wiseman, B. Gologan and R. G. Cooks, *Science*, 2004, **306**, 471–473.
- R. B. Cody, J. A. Laramée and H. D. Durst, *Anal. Chem.*, 2005, **77**, 2297–2302.
- E. S. Chernetsova, P. O. Bochkov, M. V. Ovcharov, S. S. Zhokhov and R. A. Abramovich, *Drug Test. Anal.*, 2010, **2**, 292–294.
- E. S. Chernetsova, P. O. Bochkov, G. V. Zatonskii and R. A. Abramovich, *Pharm. Chem. J.*, 2011, **45**, 306–308.
- J. L. Easter and R. R. Steiner, *Forensic Sci. Int.*, 2014, **240**, 9–20.
- M. D. Likar, G. L. Cheng, N. Mahajan and Z. L. Zhang, *J. Pharm. Biomed. Anal.*, 2011, **55**, 569–573.
- E. S. Chernetsova and G. E. Morlock, *Mass Spectrom. Rev.*, 2011, **30**, 875–883.
- M. Smoluch, P. Mielczarek and J. Silberring, *Mass Spectrom. Rev.*, 2016, **35**, 22–34.
- A. D. Lesiak and J. R. Shepard, *Bioanalysis*, 2014, **6**, 819–842.
- M. J. Pavlovich, B. Musselman and A. B. Hall, *Mass Spectrom. Rev.*, 2018, **37**, 171–187.
- J. D. Harper, N. A. Charipar, C. C. Mulligan, X. R. Zhang, R. G. Cooks and Z. Ouyang, *Anal. Chem.*, 2008, **80**, 9097–9104.
- D. N. Atecha, C. Kuhlmann and C. Engelhard, *Anal. Methods*, 2019, **11**, 566–574.
- F. J. Andrade, W. C. Wetzel, G. C. Y. Chan, M. R. Webb, G. Gamez, S. J. Ray and G. M. Hieftje, *J. Anal. At. Spectrom.*, 2006, **21**, 1175–1184.
- F. J. Andrade, J. T. Shelley, W. C. Wetzel, M. R. Webb, G. Gamez, S. J. Ray and G. M. Hieftje, *Anal. Chem.*, 2008, **80**, 2646–2653.
- F. J. Andrade, J. T. Shelley, W. C. Wetzel, M. R. Webb, G. Gamez, S. J. Ray and G. M. Hieftje, *Anal. Chem.*, 2008, **80**, 2654–2663.
- J. T. Shelley, J. S. Wiley and G. M. Hieftje, *Anal. Chem.*, 2011, **83**, 5741–5748.
- K. P. Pfeuffer, J. N. Schaper, J. T. Shelley, S. J. Ray, G. C. Y. Chan, N. H. Bings and G. M. Hieftje, *Anal. Chem.*, 2013, **85**, 7512–7518.
- G. Morlock and E. S. Chernetsova, *Cent. Eur. J. Chem.*, 2012, **10**, 703–710.
- O. Kiguchi, K. Oka, M. Tamada, T. Kobayashi and J. Onodera, *J. Chromatogr. A*, 2014, **1370**, 246–254.
- X. X. Gong, D. Zhang, I. B. Embile, Y. She, S. Y. Shi and G. Gamez, *J. Am. Soc. Mass Spectrom.*, 2020, **31**, 1981–1993.
- G. J. Van Berkel, A. D. Sanchez and J. M. E. Quirke, *Anal. Chem.*, 2002, **74**, 6216–6223.
- G. J. Van Berkel, M. J. Ford and M. A. Deibel, *Anal. Chem.*, 2005, **77**, 1207–1215.
- S. P. Pasilis, V. Kertesz, G. J. Van Berkel, M. Schulz and S. Schorcht, *J. Mass Spectrom.*, 2008, **43**, 1627–1635.
- G. Paglia, D. R. Ifa, C. P. Wu, G. Corso and R. G. Cooks, *Anal. Chem.*, 2010, **82**, 1744–1750.
- B. S. Bagatela, A. P. Lopes, E. C. Cabral, F. F. Perazzo and D. R. Ifa, *Rapid Commun. Mass Spectrom.*, 2015, **29**, 1530–1534.
- M. Heide, C. C. Escobar-Carranza and C. Engelhard, *Anal. Bioanal. Chem.*, 2022, 4481–4495.
- C. Kuhlmann, M. Heide and C. Engelhard, *Anal. Bioanal. Chem.*, 2019, **411**, 6213–6225.
- M. Ceglowski, M. Smoluch, E. Reszke, J. Silberring and G. Schroeder, *Anal. Bioanal. Chem.*, 2016, **408**, 815–823.
- A. Kim, P. F. Kelly, M. A. Turner and J. C. Reynolds, *Rapid Commun. Mass Spectrom.*, 2023, **37**, e9422.
- S. Rankin-Turner, S. Ninomiya, J. C. Reynolds and K. Hiraoka, *Anal. Methods*, 2019, **11**, 3633–3640.
- M. Rydberg, S. Dowling and N. E. Manicke, *J. Anal. Toxicol.*, 2023, **47**, 147–153.
- C. Bressan, R. Seró, É. Alechaga, N. Monfort, E. Moyano and R. Ventura, *Anal. Methods*, 2023, **15**, 462–471.
- S. A. Borden, A. Saatchi, J. Palaty and C. G. Gill, *Analyst*, 2022, **147**, 3109–3117.
- B. S. Frey, D. E. Damon and A. K. Badu-Tawiah, *Anal. Chem.*, 2022, **24**, 9618–9626.
- T. Kaser, S. Giannoukos and R. Zenobi, *J. Breath Res.*, 2025, **19**, 036002.
- D. M. Li, Z. H. Li, B. Xu, J. Chen, J. J. Xue, S. D. Hu, L. H. Wen, L. Guo, J. W. Xie and G. B. Jiang, *Analyst*, 2022, **147**, 4187–4196.
- A. Henderson, L. M. Heaney and S. Rankin-Turner, *Drug Test. Anal.*, 2024, **16**, 1323–1344.
- M. Heide and C. Engelhard, *Appl. Spectrosc.*, 2023, **77**, 928–939.
- R. Collier, *Can. Med. Assoc. J.*, 2012, **184**, E117–E118.
- H. Bahrami and H. Farrokhpour, *Spectrochim. Acta, Part A*, 2015, **135**, 646–651.
- Y. Valadbeigi, V. Ilbeigi, A. Afgar and M. Soleimani, *Int. J. Mass Spectrom.*, 2021, **470**, 116699.
- W. M. Haynes, *CRC Handbook of Chemistry and Physics*, CRC Press, 2016.

